

Manuscript version: Author's Accepted Manuscript

The version presented in WRAP is the author's accepted manuscript and may differ from the published version or Version of Record.

Persistent WRAP URL:

<http://wrap.warwick.ac.uk/167204>

How to cite:

Please refer to published version for the most recent bibliographic citation information. If a published version is known of, the repository item page linked to above, will contain details on accessing it.

Copyright and reuse:

The Warwick Research Archive Portal (WRAP) makes this work by researchers of the University of Warwick available open access under the following conditions.

Copyright © and all moral rights to the version of the paper presented here belong to the individual author(s) and/or other copyright owners. To the extent reasonable and practicable the material made available in WRAP has been checked for eligibility before being made available.

Copies of full items can be used for personal research or study, educational, or not-for-profit purposes without prior permission or charge. Provided that the authors, title and full bibliographic details are credited, a hyperlink and/or URL is given for the original metadata page and the content is not changed in any way.

Publisher's statement:

Please refer to the repository item page, publisher's statement section, for further information.

For more information, please contact the WRAP Team at: wrap@warwick.ac.uk.

Design, Build and Retrofit of a 20 kW Automotive Wireless Charging System using CCS Interface

Alex Ridge

WMG, University of Warwick
Coventry, UK
a.ridge@warwick.ac.uk

Silvia Konaklieva

WMG, University of Warwick
Coventry, UK

Ku Ku Ahamad

WMG, University of Warwick
Coventry, UK

Sul Ademi

WMG, University of Warwick
Coventry, UK

Shivam Mishra

WMG, University of Warwick
Coventry, UK

Jianguo Wang

WMG, University of Warwick
Coventry, UK

Richard McMahon

WMG, University of Warwick
Coventry, UK

Abstract—This paper presents a case study of the full development process from modelling and design to build, vehicle integration and testing of a 20 kW rated wireless charging system. The combined charging system (CCS) DC charging interface on the vehicle was used for vehicle charging and communication. The work motivation along with details of the system design, construction and vehicle integration are included in this paper. The main learning points are discussed and test results showing the final system in operation are presented.

Index Terms—Wireless power transmission (WPT), inductive charging, vehicular and wireless technologies, automotive applications, charging stations, CCS charging.

I. INTRODUCTION

The work reported in this paper has been motivated by the participation in a UK local authority led project on lowering carbon emissions, which includes the promotion of electric vehicles (EVs) and the upgrade of supporting EV charging technologies [1]. By removing the need for a charging cable, wireless charging is seen as very promising in terms of improving charging convenience (particularly for those less physically able to handle large cables), reducing street clutter/trailing cables and thus also improving overall pedestrian safety. A public demonstration system has been commissioned to engage with potential users and gauge their interest in wireless charging technology.

The principle specifications for the commissioned system are a power rating in the range of 10-20 kW and for the system to be retrofitted to one of the popular EV models. A BMW i3 was selected and obtained for this purpose. Furthermore, a mobile ground assembly (GA) was requested so that the system can be demonstrated in more than one public location without the need for ground installation - an above ground mounted GA pad is therefore used. The power supply to the GA electronics is from a 32A 3-phase mains socket available at the intended demonstration locations. Aligning with the emerging wireless charging standards [2], [3], an 85 kHz operating frequency is chosen along with the common unipolar square topology for the GA and vehicle assembly (VA) pads.

II. SYSTEM DESIGN AND CONSTRUCTION

A. Wireless pads

The wireless pads were designed and briefly optimised using COMSOL Multiphysics software. A number of aspects were explored during the optimisation stage, including variation of coil/ferrite width and length, coil winding width, and shielding design. The design magnetic gap between the coils ranges from 90 to 120 mm (corresponding to an above-ground mobile GA pad) and the horizontal offset is up to 75 / 100 mm (X/Y). The target was to establish a reasonable coupling coefficient between the pads whilst also aiming to keep the stray magnetic field beyond the area immediately underneath the car below the ICNIRP 1998 public limit (this limit is below those in the emerging wireless standards [2], [3], but most relevant to UK public spaces [7]). To examine stray field levels and also set the number of turns / final ferrite thickness, the required currents in the wireless pads were estimated for this project based on the required power levels, modelled pad parameters and a modest loaded secondary resonant Q of 3. The number of turns were semi-arbitrarily set to keep the terminal voltages of the pads within a 1-1.5 kV rms range for ease of voltage insulation and measurement. Due to time pressures on the project, wireless pad build had to commence before the resonant circuits were designed, hence the use of these approximations. The overall wireless pad dimensions are:

- Ground pad: 710 x 710 x 40 mm
- Vehicle pad (square part): 450 x 450 x 34 mm

The pads are constructed using Litz wire backed by 100 x 100 x 8 mm, BH1T ferrite plates. They were potted with an AEV Ltd custom-made epoxy-type resin selected for thermal conductivity and strength. The vehicle pad has a trapezoidal protrusion on the side of the cable glands to accommodate the butt splice crimps connecting the Nomex-insulated inner Litz wire coil and its outer extensions with automotive-grade insulation. The ground pad due to its overall larger dimensions does not need such extra crimp space. Fig. 1, illustrates the ground and vehicle pads pre- and post potting.

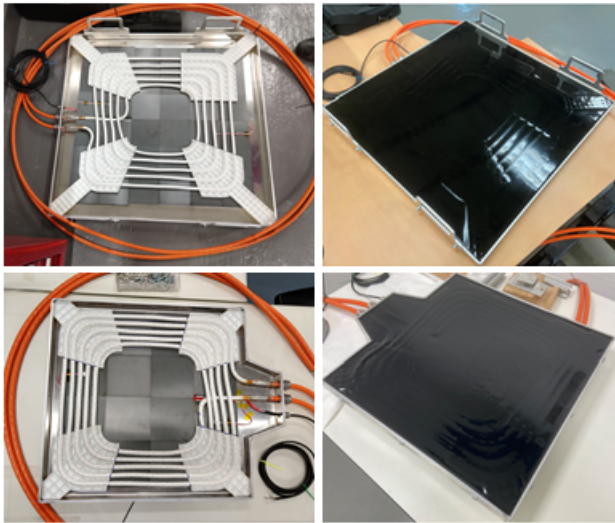


Fig. 1. Ground pad construction photos (above); Vehicle pad construction photos (below).

Measured parameters across the desired operating range, including the effect of 5 m and 2.5 m Litz extension cables on the primary and secondary pads respectively, show primary inductances between 23 and 25 μH , secondary inductances between 18 and 19 μH and coupling coefficients between 0.12 and 0.27. Measurements before potting indicated that the Litz extension cables (loosely twisted) had added 0.6 μH per meter of extension to the self-inductance of the bare pads.

B. Resonant Circuit

An LCC-LCC compensation topology configured for constant current control feedback is selected for the resonant circuit as it provides more degrees of freedom than the other commonly used topologies (such as the simpler series or parallel compensation). The design aim was for the system to appear slightly inductive across the full operating range of wireless pad parameters, battery voltage and power levels, allowing the inverter to operate with zero voltage switching (ZVS) while delivering the required power output [4], [5]. Additional aims of establishing a reasonable loaded secondary Q and avoiding significant sensitivity of the resonant circuit to component value variations were also targeted. The LCC-LCC inductor and capacitor values were optimised using MATLAB scripts. These scripts used analytical equivalent circuit equations to evaluate a large range of candidate resonant circuit designs, each against the full range of pad inductance/coupling coefficient values and system supply/load voltage/power specifications. The results of these computations were used to trade-off a number of electrical parameters with the overall aim described above and the final resonant circuit design was verified using time-domain simulations in PLECS. The final resonant circuit component values are shown in Table. I.

The resonant inductors for both primary and secondary compensation circuits were constructed using Litz wire and 3C94 ferrite E-cores, with an appropriate air gap selected to

TABLE I
RESONANT CIRCUIT COMPONENTS VALUES

Component	Target value	Measured
Primary side inductor	12.4 μH	11.99 μH
Primary series capacitor	621nF	620nF
Primary parallel capacitor	283nF	284nF
Secondary side inductor	6.2 μH	6.05 μH
Secondary series capacitor	548nF	550nF
Secondary parallel capacitor	644nF	650nF

control the flux in the core. The resonant capacitor banks were constructed with a number of series and parallel capacitors (of the Multicomp Pro Metallized PP line) chosen for their compact overall volume combined with a high resulting nominal voltage rating. One drawback of these capacitors is the fact that their live bus bars need heat sinking which required use of additional ceramic insulation and thermal epoxy for securing the capacitor bank. The GA and VA resonant circuit components can be seen in Fig. 2 (with the exception of the VA side inductors). For symmetry the inductors and the series capacitors of the LCC circuits have been split in two physical components.

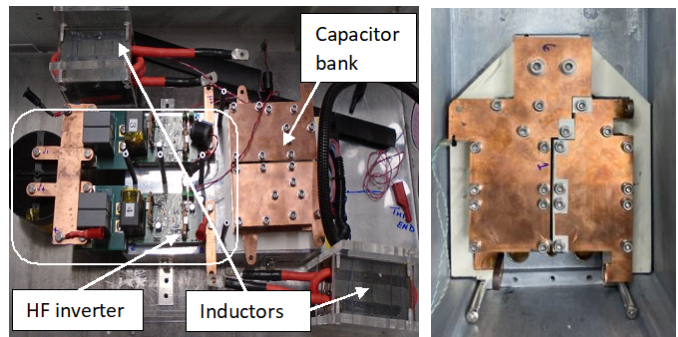


Fig. 2. (Left): GA Electronics box during construction. (Right): VA Electronics box during construction showing resonant circuit capacitors glued to a ceramic substrate on the bottom of the box

C. Inverter and Rectifier

The primary side is driven by a H-bridge inverter developed for the purpose, fed from a DC source. The inverter is constructed using BSM300D12P2E001 ROHM SiC power modules together with an in-house developed gate driver circuit. The operating frequency of 85 kHz was used. The output from the secondary compensation circuit is passively rectified into a DC link. A passive rectifier was chosen to minimise complexity on the vehicle side electronics. It comprises DCG130X1200NA SiC Schottky diode packs in a full-bridge configuration and a metallised can power film DC link capacitor MP003985 supporting ripple at frequencies in excess of double the system operating frequency.

D. Control and Internal Communications

In order to charge an electric car using DC, closed-loop control of the system output is needed. In essence, the Battery

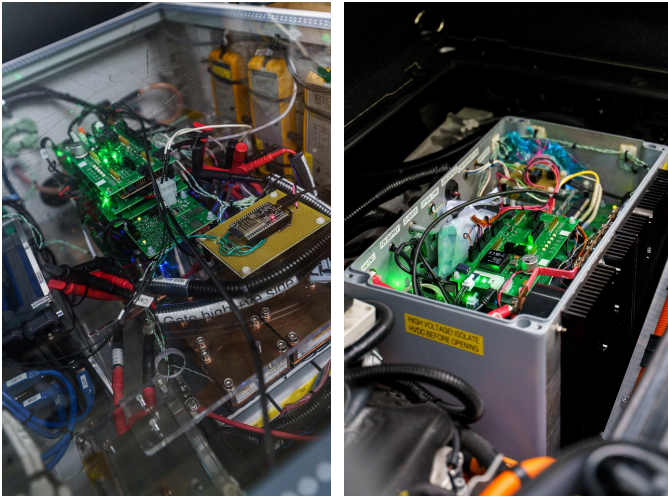


Fig. 3. (Left): Completed GA Electronics box showing resonant circuit, control boards, and some probes for external monitoring. (Right): Completed VA Electronics box showing control boards and side-mounted rectifier (resonant circuit underneath control boards)

Management System (BMS) in the car will set charging current and output voltage limits during the charging process which must be adhered to by the wireless system. An overview of the control and power components of the wireless system is shown in Fig. 4. Control of the system output is via the ground-side, specifically by adjusting the DC input voltage to the high-frequency inverter. DC input voltage control was chosen here over inverter duty-cycle control for simplicity and speed of system development. A set of monitoring and control circuit boards have been developed in-house to realise the sensing, control and communications requirements for the overall system. These consist of:

- DC measurement of voltage and current - based around the TI AMC 1200/1300 series of isolation amplifiers
- 85 kHz AC measurement of primary and secondary coil currents - based around isolation amplifiers and the Analog devices AD8436 RMS to DC conversion chip
- Temperature measurement of system components using the Maxim MAX31855/MAX31865 chips
- Gate drivers based around the Murata MGJ6 series of isolated DC/DC converters and TI UCC53x0 chips
- TI C2000 F28379D microcontrollers, one on each side of the system - conveniently available in a TI 'LaunchPad' form for this prototype system and featuring CAN, SPI, Serial, ADC and PWM peripherals
- A set of Kvaser AirBridge CAN-over-Wifi adapters providing a wireless comms link between GA/VA controllers
- An ESP32 wifi-enabled microcontroller on the ground side which provides connectivity to a mobile device allowing users to start, stop and monitor charging activity

E. CCS-based Vehicle Communication

Due to the popularity of CCS-based DC charging in Europe, the wireless system was developed to use this method

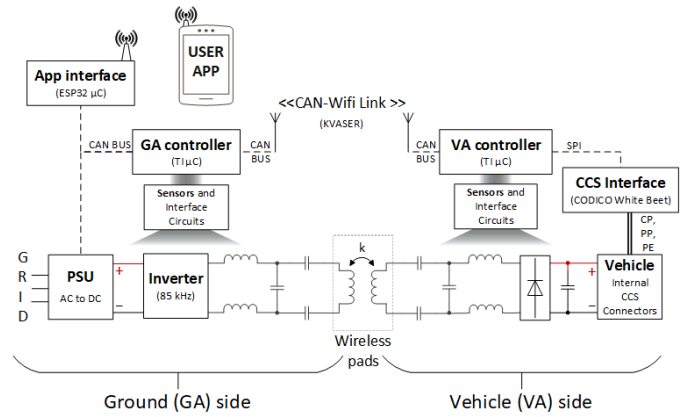


Fig. 4. System overview

to communicate with the vehicle and manage the charging process. By mimicking a regular DC charging post, OEM-level integration is avoided and the solution is car-manufacturer agnostic. It is acknowledged that specific communications protocols are in development to support wireless charging, including ground to vehicle wireless communications [6]. The approach utilised here is applicable here-and-now and retrofittable to existing electric vehicles as was required for this project.

Briefly, CCS DC vehicle charging involves the following:

- 1) Initiating the communication via the PP and CP lines, using 5% PWM to indicate high-level communications
- 2) Establishing power-line communications (PLC)
- 3) Negotiating charging session parameters with the vehicle and performing safety checks
- 4) A pre-charge phase whereby the DC voltage output of the system is ramped to a value requested by the vehicle
- 5) Vehicle contactors closed by the vehicle
- 6) A charging phase whereby the DC current is regulated according to values requested by the vehicle
- 7) Upon charge completion or stop request, a post-charge phase including welding detection for the contactors.

A CODICO® White Beet module [8] is utilised to help integrate the PLC-based CCS communication. This module includes a PLC modem, hardware to manage the CP line, and an internal microcontroller which handles a portion of the CCS-based communications. The module exposes a documented API over SPI or Ethernet, allowing other systems (the VA-side TI microcontroller in our case) to interface with it. The API documentation includes a list of commands, requests and required responses to achieve a complete charging session - these were suitably integrated into our control system.

The following aspects were noted during our particular project and are included here to help future researchers / system builders: Within CCS there are multiple protocols that can be supported, such as DIN 70121 and ISO 15118. During charging phases, output voltage and current measurements are repeatedly requested by the vehicle along with a timeout during which the request message must be answered. In

our case, the shortest timeout was approx 70 ms. Current requests are repeatedly supplied and dynamically adjusted by the vehicle during charging. The DC current request from the vehicle during charging could be regarded as an upper limit, allowing gradual adjustment of charging current towards this level. If the vehicle is not satisfied with responses from the charging system it will request termination of the charging session. As with any system, safety and potential failure modes must be considered during the design stage. A suitable response to charging system errors may include stopping the power transfer and also actively issuing a stop response to the vehicle over CCS so that the vehicle will also open its contactors / go through its post-charge sequence.

III. VEHICLE INTEGRATION

One of the more challenging aspects in the design and build of this wireless charging system was its vehicle integration and retrofit. The mechanical integration (subcontracted to specialists) involved scanning of the vehicle undercarriage and identifying favourable mounting positions for the vehicle pad. The pad is secured in place via an aluminium riff-bonded structure made of extruded profiles sandwiched between sheet metal using existing fixing points on the bottom of the BMW i3's battery tray (also aluminium).

The structure was designed with a front slope to allow a more aerodynamic flow of air under the vehicle in motion. The pad and holding structure (with total weight 38 kg) underwent software modelling for load cases modal to 200 Hz and 5g vertical bump prior to installation yielding maximum displacement and stress level within target.

While current draft wireless charging standards specify a forward position for the wireless charging pad, in this project it was desirable to allow users to park either forwards or in reverse as they would normally. For this reason, a centre-mounted pad position is used. Fig. 5 illustrates the selected pad-mounting position and Fig. 6 shows the finished underside of the BMW i3.

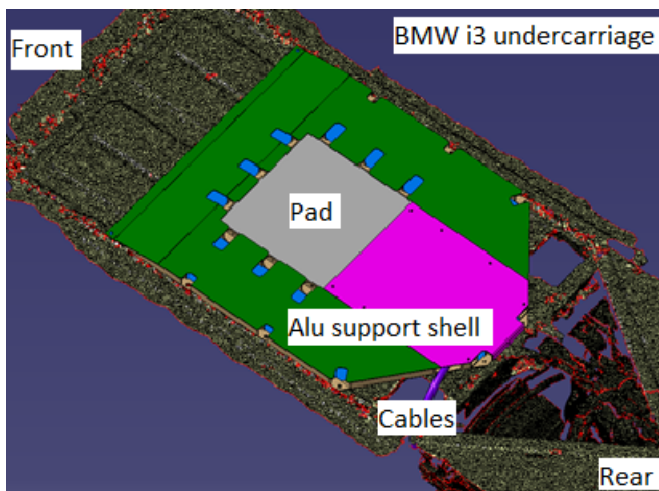


Fig. 5. Pad and support structure. [Credit: Corum Technology]



Fig. 6. Pad and support structure fitted on the BMW i3 undercarriage.

The housing of the vehicle electronics box inside the BMW i3 presented another challenge in terms of mechanical integration. It was decided to fit it “engine-side” rather than “cabin-side” to conserve vehicle boot space for the safety and convenience of the public demo target audience and this was enabled by utilising the available free space normally occupied by the range extender used in the hybrid i3 models. Nevertheless, this restricted the size of the electronics box enclosure. A Rose Aluminium Standard die cast enclosure 400 x 230 x 225 mm was selected for this purpose with additional externally bonded heat sinks. Fig. 7 shows the opened vehicle electronics box. It can be seen that the components inside it are layered in several levels with a perspex separation between the heavier bottom-lying resonant circuit and the sensor and control electronics. The physically lighter HF rectifier is mounted on the side of the enclosure.

The box is mounted on a support structure as illustrated in Fig. 8 with the pad cables entering it from bottom left-hand side as seen from above and the DC cable glands on the front forward facing side.



Fig. 7. Vehicle box internal architecture during construction, showing the layer approach and side-mounted rectifier.

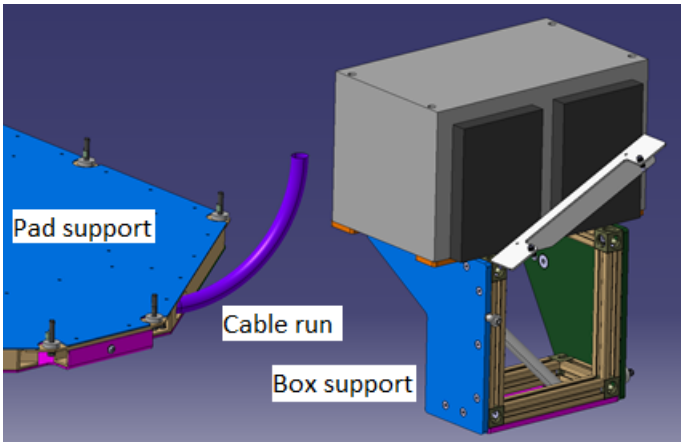


Fig. 8. Pad and vehicle electronics structure. [Credit: Corum Technology]

For electrical integration of the wireless charging system, the DC cables to the vehicle's CCS charging socket were disconnected from the vehicle's internal connector and the output of our system plugged in instead. A spare charging harness was acquired from which the appropriate automotive connector was sourced. A switchable relay-controlled connection of the PP and CP signal wires exists within the vehicle box to retain plug-in AC charging ability for the vehicle when the wireless charging system is not active. Fig. 9 illustrates the vehicle box retrofit being finalised.



Fig. 9. Vehicle with fitted electronics box in the process of finalising the electrical and comms systems integration.

The vehicle retrofit process aimed to preserve the BMW i3's electrical and mechanical integrity, minimise the impact of the changes on the vehicle and allow full reversal back to its pre-retrofit state once the wireless charging system is decommissioned and removed.

IV. TESTING AND RESULTS

Testing of the system during development was key to both identifying issues early and giving confidence to progress to

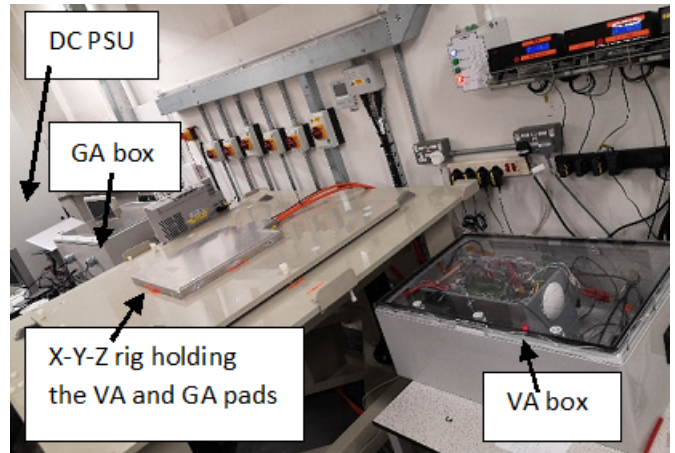


Fig. 10. Lab test set-up showing most of the major system sub-assemblies.

the next stage. In our project the system was first tested open-loop on a lab bench with a resistive load up to the target 20 kW. Next was a "vehicle-in-the-loop" test during which the vehicle's battery was charged (over a CCS cable connection from the wireless system to the vehicle). Full vehicle integration was then completed with final rounds of testing.

Fig. 10 highlights some of the major parts of the lab bench test setup. Out of view of this figure was the system load (resistive load bank or the vehicle itself) and an array of oscilloscopes for monitoring the main signals of interest.

Wireless power transfer of close to 20kW was demonstrated using a resistor load bank as a DC sink with output signals after the rectifier: DC voltage of 356V and DC current of 55A as shown in the oscilloscope screenshot of Fig. 11.

Wireless power transfer into the vehicle battery was also tested in this setup, with Fig. 12 showing the voltage and current signals supplied to the vehicle battery during one of the tests. This test shows power transfer of 10 kW into the

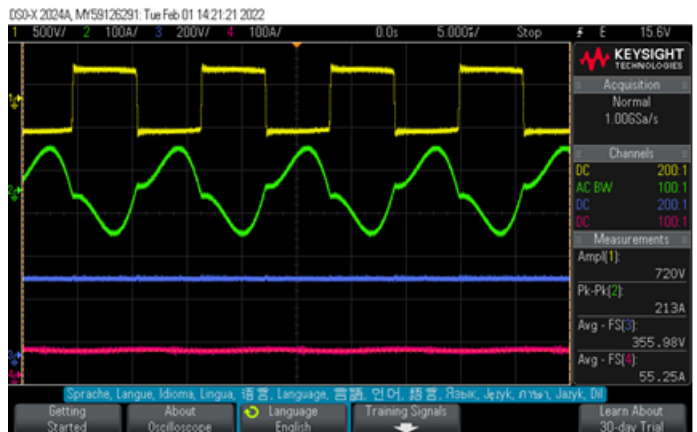


Fig. 11. Oscilloscope screenshot showing the AC voltage into the rectifier (yellow), the AC current into the rectifier (green), the DC voltage out (blue) and the DC current out (magenta).

vehicle battery which was sufficient to meet the requirements of this particular project. Due to time pressures and a desire to be relatively cautious so as to deliver reliable public demonstration, power transfer to the vehicle has been tested up to 10 kW to date. Extending this to 20 kW to match power levels demonstrated in the resistive load tests is left for future work.

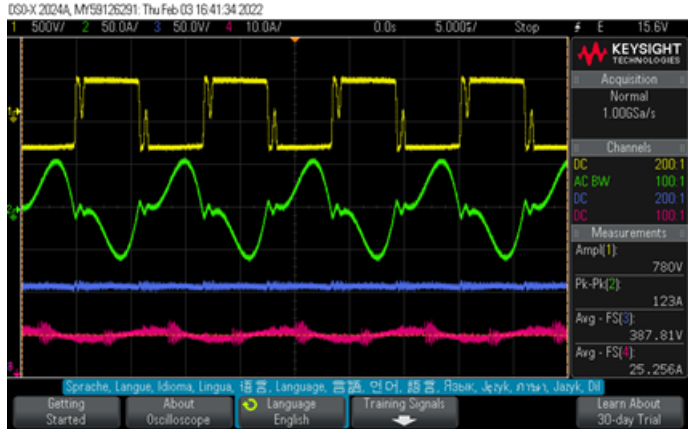


Fig. 12. Oscilloscope screenshot showing the AC voltage into the rectifier (yellow), the AC current into the rectifier (green), the DC voltage out to the EV battery (blue) and the DC current out to the EV battery (magenta).

Following full vehicle integration a more comprehensive series of tests were conducted at different vehicle alignments, battery states of charge and power levels. At 10 kW of power transfer to the vehicle, the corresponding DC link measurements on the primary side vary from 265 V / 40 A in a fully-aligned configuration to 470 V / 23 A at an X/Y offset of 100/100 mm (slightly larger than the 75/100 mm offset requirement). This is in agreement with system simulations during the design stage and a good match to capabilities of the intended DC power supply. DC-to-DC system efficiency at 10 kW was measured at between 90 and 95 %, and AC-DC efficiency of the power supply used is quoted at 95 %. Stray magnetic field levels are measured to be below the 6.25 μT ICNIRP 1998 public exposure level in all areas that a human can reasonably access (i.e. everywhere except underneath the vehicle), as targeted during the design stage. Temperature rises observed in the final system were well within component ratings.

During real-world public demonstration activities of the project to date, the system has performed reliably and within expected operating targets. To aid vehicle alignment, simple mechanical means were employed consisting of a wheel bumper and either an alignment sign to aim at (for forward parking) or strips on the road (for reverse parking). The vehicle did not have parking cameras. Following a brief explanation, participants new to the project were mostly able to park the car within the required alignment on their first attempt. As previously mentioned, an app running on a mobile device was also developed to allow users to start / stop / monitor charging activity - this was much appreciated by the participants and

formed a large portion of the user experience of the system. Fig. 13 shows the demonstration activity.



Fig. 13. Public mobile demonstration showing vehicle approaching wireless

V. CONCLUSION

This paper has presented the design and build of a 10-20 kW wireless charging system including retrofit with a commercial EV using the CCS charging interface. The system was shown to be reliable and to meet all the principle design targets of power level, misalignment tolerance, stray field levels and user experience. While the design process has been briefly summarised in this paper, the main contribution is viewed as a case study of taking a system from a lab bench proof-of-concept stage to complete vehicle integration. Details of how the system was realised and how the vehicle integration was achieved have been included with the intention of being informative for future researchers.

The design has scope for further optimisation - potentially for future manufacture. Working with manufacturers and forming supply chains for wireless charging systems are of active interest.

REFERENCES

- [1] D. Hirst, N. Dempsey, P. Bolton, and S. Hinson, "Electric vehicles and infrastructure," House Commons Libr., no. CBP07480, 2020.
- [2] SAE International, "J2954, Wireless Power Transfer for Light-Duty Plug-in/Electric Vehicles and Alignment Methodology," 2020.
- [3] IEC, "61980, Electric vehicle wireless power transfer (WPT) systems," 2019/2020.
- [4] S. Li, W. Li, J. Deng, T. D. Nguyen, and C. C. Mi, "A Double-Sided LCC Compensation Network and Its Tuning Method for Wireless Power Transfer," *IEEE Trans. Veh. Technol.*, vol. 64, no. 6, pp. 2261–2273, 2015.
- [5] Y. Chen, N. Yang, Q. Li, Z. He, and R. Mai, "New parameter tuning method for LCC/LCC compensated IPT system with constant voltage output based on LC resonance principles," *IET Power Electron.*, vol. 12, no. 10, pp. 2466–2474, 2019.
- [6] ISO, "15118-8, Road vehicles - Vehicle to grid communication interface - Part 8: Physical layer and data link layer requirements for wireless communication," 2020.
- [7] National Grid, "Limits in the UK", <https://www.emfs.info/limits/limits-uk/>, accessed 2022
- [8] CODICO GmbH, "WHITE-BEET-EI (EVSE) Embedded ISO15118 Module", <https://www.codico.com/en/white-beet-ei-evse-embedded-iso15118-module>, accessed April 2022